Pathways to charge equilibration following multiple electron exchange between highly charged ions and atoms

de Nijs, Gerardus

Chapter 4

A coincidence study of multiple-electron capture in $^{15}N^{7+}$-Ar collisions

Abstract *We present energy spectra of autoionization electrons resulting from collisions between fully stripped $^{15}N^{7+}$ ions and Ar in the energy range of 1-10 keV amu^{-1}. These spectra were measured in coincidence with charge-state analyzed Ar ions. Observed populations of the various configurations are discussed in the framework of the classical overbarrier model. Our measurements suggest that target-ion excitation together with two-electron capture is an important process in collisions between bare N^{7+} ions and Ar. We find evidence that radiative stabilization of doubly excited $N^{5+}(4l, 4l')$ states is even stronger than was thought up till now.*

4.1 Introduction

If a highly charged ion collides on a gas target, electrons are transferred from the target to the ion and are captured in highly excited states of the ion. The resulting multiply excited ions will decay radiatively or by autoionization. For autoionization at least two electrons are needed, so in an electron spectrum resulting from collisions between highly charged ions and a two-electron gas target (e.g. He or H_2) the detected electrons are due to two-electron transfer. The main features of such autoionization electron spectra (e.g. Mack and Niehaus 1987, Mack 1987b, Bordenave-Montesquieu *et al* 1987) can be understood in the framework of the semi-classical overbarrier model (Niehaus 1986, Posthumus *et al* 1992), where quasi-resonant capture is assumed.

Spectra from more than two-electron capture processes are more difficult to understand because the measured spectra are generally a superposition of

components, resulting from different capture processes. A measured electron can in principle originate from a two-electron as well as from a multi-electron capture process. To distinguish between these alternatives it is necessary to measure the autoionization electron in coincidence with the number of electrons transferred from the gas target to the highly charged ion.

We can measure the emitted electrons in coincidence with the resulting charge state of the target (Posthumus and Morgenstern 1992a), enabling the determination of the electron spectra corresponding to specific numbers of captured electrons. In this chapter we present the first coincidence measurements between energy-analyzed autoionization electrons and the charge state of the target for collisions of fully stripped N^{7+} ions and Ar. The coincidence measurements are performed at three different collision energies, 2.3, 4.7 and 8.9 keV/amu. Non-coincident electron spectra were measured in the energy range of 1-10 keV/amu.

We used bare N^{7+} ions as projectile ions because the energy levels of the final N^{6+} ions are degenerate, thus facilitating the analysis of the spectra. For Ar as a target the classical overbarrier model predicts a dominant population of $N^{5+}(4l, 4l')$ projectile states for the case of two-electron capture. Since the (4,4) manifold partly overlaps the $N^{5+}(3l, nl')$ Rydberg series one can expect an interaction between these different configurations. Such an interaction has been discussed recently (Bachau *et al* 1992, Roncin *et al* 1993,Vaeck and Hansen 1993) as giving rise to radiative stabilization of the captured electrons.

Benoit-Cattin *et al* (1988) have investigated multiple-electron capture in collisions between N^{7+} on Ar from the measured singles electron spectra. Their conclusions, based on the observed electron spectra, can now be tested. We will show in this chapter that an unexpected broad spectrum of states results from two-electron capture, ranging from (3,3) to (3,n) states with $n > 10$ as well as (4,4) and (4,5) states. We will show that populating the (3,4) states is probably accompanied by simultaneously exciting an electron in the target.

4.2 Experiment

Details of the experimental method are discussed in chapter 3. Here only the most important points will be summarized. Highly charged fully stripped $^{15}N^{7+}$ ions are extracted from an ECR-ion source (see e.g. Geller and Jacquot 1982) installed at the KVI Atomic Physics facility. The source can operate at voltages between 2 and 20 kV. After mass/charge selection the N^{7+} ions are transported to our setup in which they can collide with an Ar gas target. Collision products are observed by two spectrometers. Firstly in forward direction there is a cylindrical electrostatic mirror analyzer (CEMA) used as electron spectrometer, which accepts electrons ejected in the laboratory frame under an angle of $50.0 \pm 2.4^{\circ}$ (Mack 1987a, b), secondly in backward direction there is a target ion charge state spectrometer (Posthumus 1992, Posthumus and Morgenstern 1992b) which detects the ions on a channeltron detector after extraction of these ions from the reaction center by means of a small voltage. During the collision electrons are transferred from Ar to $^{15}N^{7+}$. The charge state of the resulting Ar ion,

and thus the number of the electrons initially transferred to the bare nitrogen ion, is derived from the time-of-flight (TOF) of the ions. Detection of an emitted electron and of an Ar ion serves as start and as stop of the TOF measurement, respectively. For each registered coincidence event the corresponding electron energy and ion TOF are stored in a personal computer, which also controls the experiment.

The target gas pressure is kept low: $\leq 8 \times 10^{-5}$ Pa for singles measurements and $\sim 2 \times 10^{-5}$ Pa for coincidence measurements. The background pressure is about 8×10^{-6} Pa. The typical beam current on target is ≤ 1 nA during coincidence measurements, while for the non-coincidence measurements (singles) the beam current is typically $\sim$6 nA. Isotopic $^{15}N^{7+}$ ions were used as projectiles to avoid contamination of the beam with $^{4}He^{2+}$ which is used as a mix gas in the ECR-ion source as would occur using $^{14}N^{7+}$-ions.

The count rate was about 0.25 events per second during coincidence measurements and about 2 events per second during singles measurements. The count rate for detecting an electron is much lower than the count rate for detecting a target ion, because electrons are strongly selected according to emission angle and energy, whereas nearly all resulting ions are extracted and guided to the ion detector.

4.3 Experimental results

In figure 4.1 we show a comparison of singles electron energy spectra for collisions of N^{7+} on Ar and on H_2 respectively. If only two-electron capture processes were important one would expect similar spectra since the sum of the first two ionization potentials of Ar and H_2 are similar: 43.4 and 50.9 eV respectively. The comparison between these spectra therefore directly demonstrates the importance of many-electron processes in case of the Ar target.

The singles measurements were done at the following collision energies: 17.5, 21, 28, 35, 42, 49, 56, 70, 84, 98 and 133 keV. In figure 4.2 we show some typical singles electron spectra for 35, 56 and 133 keV. The spectra are corrected for Doppler shifts and for the energy dependent transmission of the spectrometer $\Delta E/E$. For the singles only a constant background is subtracted from the raw data. In these spectra one can observe in the range of 70 to 95 eV that as function of the energy the intensities of the peaks, indicated as (3,5) to (3,9), changes with respect to the peak, indicated as (4,4). This energy dependence can be seen from the ratio $I(4,4)/[I(4,4)+\sum_{n>4} I(3,n)]$, where $I(n_1,n_2)$ is the intensity of a peak indicated as (n_1,n_2).

This ratio is plotted in figure 4.3. As function of the collision energy we observe that the relative intensity of the region indicated as (4,4) first increases and then decreases. Apparently this dependence is influenced by several effects, which, however, are not yet understood in detail.

In figure 4.4 we show the results for 70 keV N^{7+} on Ar as an example of the coincidence measurements. The vertical axis of the scattergram represents the ion time-of-flight, the horizontal one the electron energy. Above the horizontal

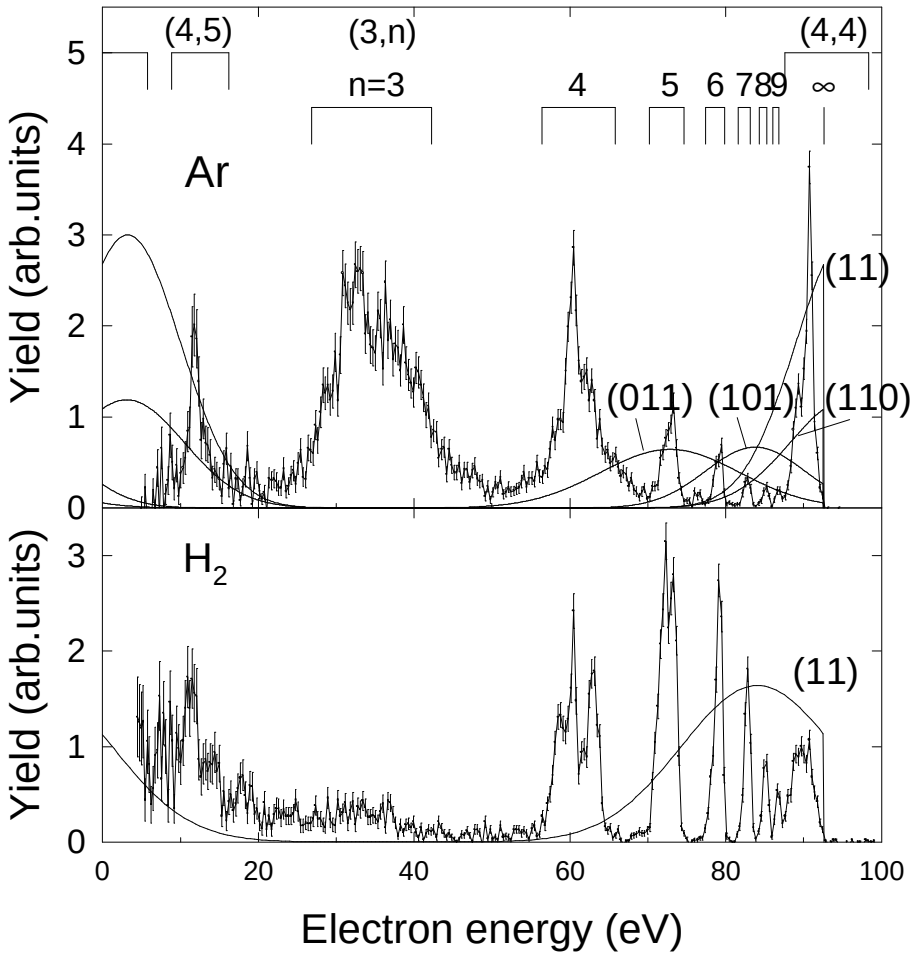

Figure 4.1: Electron spectra from collisions of 70 keV $^{15}N^{7+}$ on Ar and on H_2. The full curves are the reaction windows for the two collision systems. Note that the higher binding energy of the two electrons shifts the reaction window for H_2. On top the energy positions of different (n_1, n_2) configurations are indicated. Differences in the spectra are mainly due to the possibility of many-electron capture from the Ar-target.

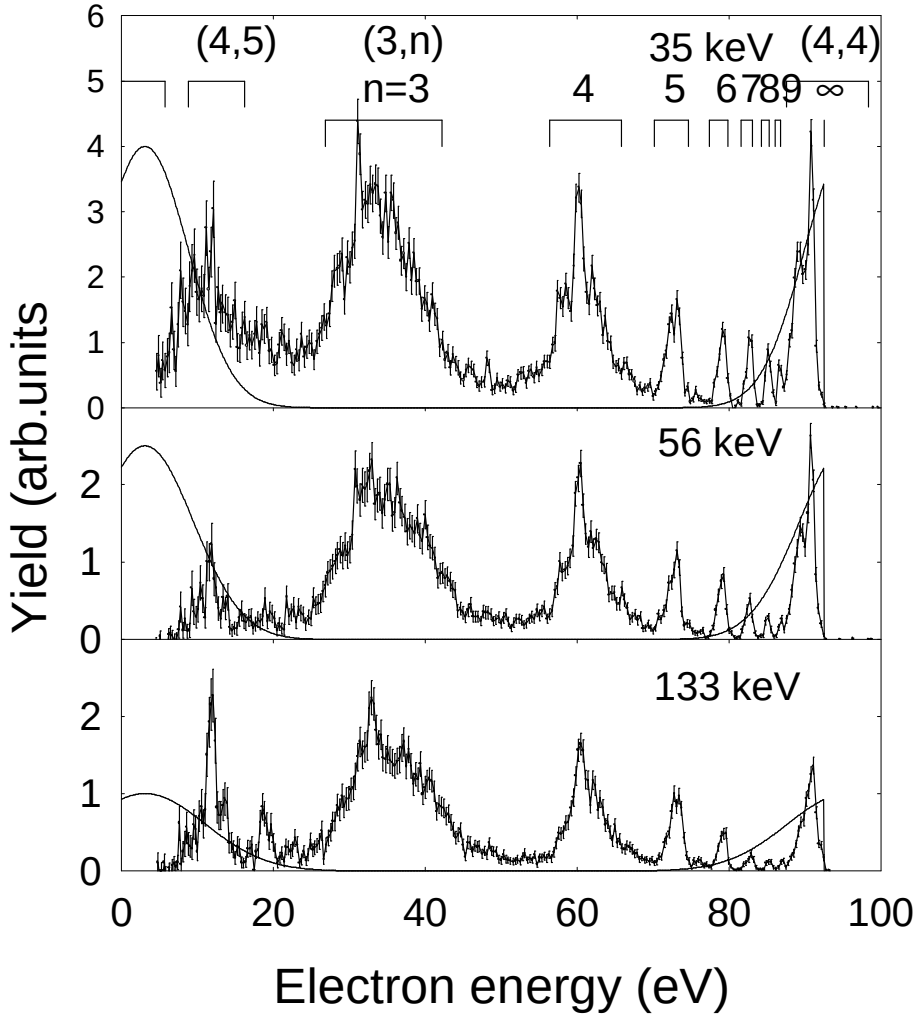

Figure 4.2: Singles electron spectra arising from N^{7+}+Ar collisions at different collision energies. In each spectrum the reaction window for capture of the two most loosely bound electrons is plotted.

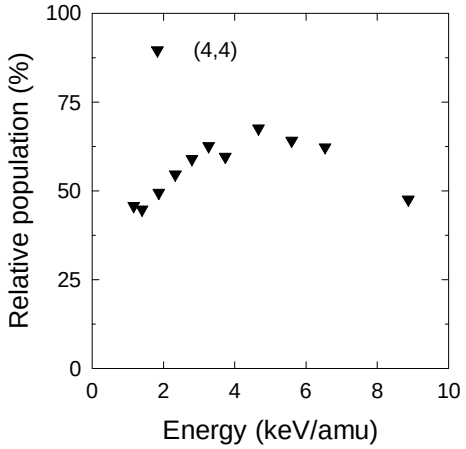

Figure 4.3: Measured relative intensity of the peak indicated as (4,4), with respect to the sum of the peaks between 70 eV and 90 eV indicated as (3,n) cf. figure 4.1

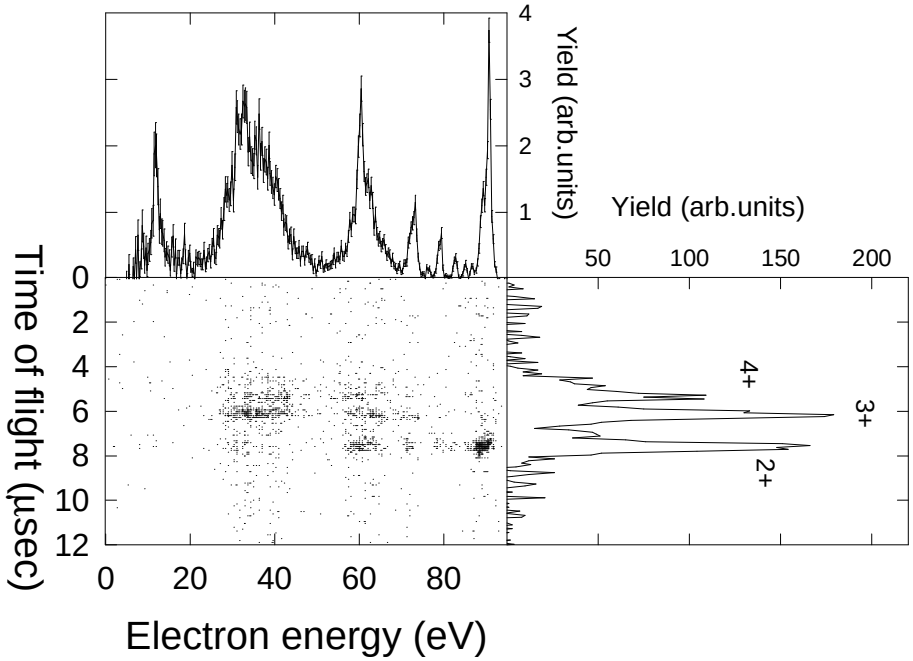

Figure 4.4: An example of the coincidences scattergram measured at 70 keV collision energy. Each dot in the picture means that at least two coincidence events are measured. Clustering of dots indicates true coincidences. Above the scattergram the non-coincident electron spectrum is plotted. At the right the time-of-flight spectrum of the target ions is plotted.

axis the singles spectrum is plotted. Each coincidence event is represented by a small dot in the scattergram. Clustering of these dots indicates true coincidences. From each spectrum the background is subtracted. The background subtraction method is as follows: the coincidence scattergram is divided into small electron energy regions of 0.5 eV. Per 0.5 eV energy region a summed time-of-flight spectrum is determined. A linear function is fitted to this summed spectrum to obtain the background, i.e. the accidental coincidences. Of course, that part of the spectrum where true coincidences appear ($\sim$4-9 μsec, cf. figure 4.4) is not included in the background fitting procedure. The background function is then subtracted from the time-of-flight spectrum.

Resulting electron energy spectra with the number of transferred electrons as parameter can now be obtained from the background corrected scattergram by placing gates around the flight times of target ions with charge states corresponding to the number of transferred electrons. Electron energy spectra in coincidence with 2+, 3+ and 4+ Ar-ions are shown in figure 4.5 for collisions of 35 keV and 70 keV $^{15}N^{7+}$ on Ar.

4.4 Discussion

4.4.1 General

Schematically the processes investigated are described by

$$N^{7+} + Ar \rightarrow (N\ Ar)^{7+} \rightarrow N^{(7-t)+} + Ar^{r+} + (r-t)e^{-} \qquad (4.1)$$

where r is the number of transferred electrons, t the number of captured electrons, and thus $r-t$ the number of emitted electrons.

We will discuss the different electron capture processes in the framework of the classical overbarrier model (Niehaus 1986, see also chapter 2). The model predicts binding energies, principal quantum numbers and cross sections for the different processes. Furthermore it provides reaction windows. These Gaussian shaped windows give the range around the most probable central binding energy where capture mainly takes place. The width of a reaction window is proportional to the square root of the collision velocity. The overbarrier model uses so called strings to label the different processes. For example a string {1010} means that four electrons become quasi-molecular during the collision and that the first and third one are captured ('1') by the projectile ion, while the second and fourth are recaptured ('0') by the target ion. In the calculations for the N^{7+} on Ar case, we assume that at most five electrons participate in the collision processes. This maximum number is based on the fact that in the coincidence measurements (see figure 4.4) we see no evidence that more than four or maybe five electrons are being transferred.

In first approach we used, following Posthumus and Morgenstern (1992b), only the so called outer strings for calculating the reaction window. These strings reflect processes where all the electrons which become quasi-molecular

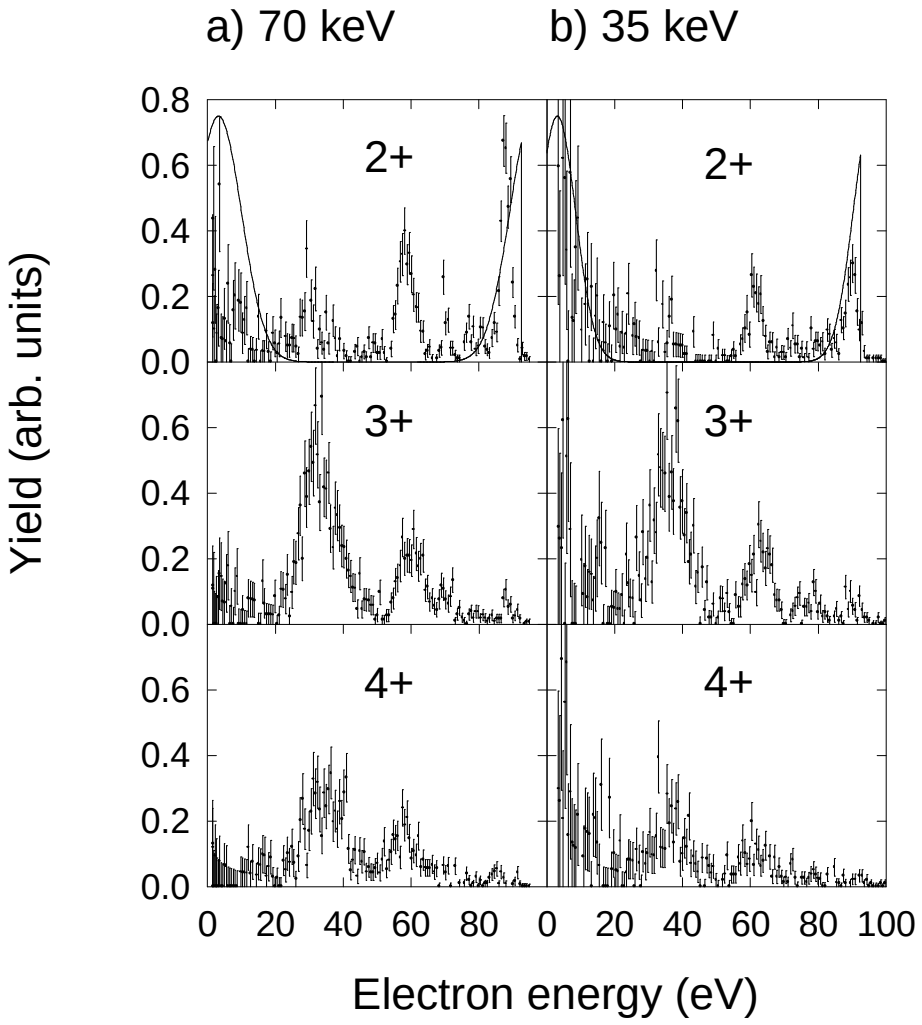

Figure 4.5: Partial electron spectra for two-, three- and four electron transfer in (a) collisions of 70 keV $^{15}N^{7+}$ on Ar and (b) 35 keV $^{15}N^{7+}$ on Ar. The spectra are Doppler shift and spectrometer transmission corrected. In the upper panels the reaction window for the two most loosely bound electrons are plotted.

during the collision, are captured by the projectile. These strings are denoted e.g. by {11} for two-electron processes or {1111} for four-electron processes.

The most probable binding energy E_c can be converted into a principal quantum number $n_c = q/\sqrt{2E_c}$, which in the first place is regarded as a continuous quantity. To get an estimate of the most probable principal quantum number we ascribe an integer n to each electron in a string which fulfills the relation:

$$[(n-1)(n-\frac{1}{2})n]^{\frac{1}{3}} \leq n_c \leq [n(n+\frac{1}{2})(n+1)]^{\frac{1}{3}} \qquad (4.2)$$

(Olson 1981).

The configurations which will be populated are actually those which lie inside the calculated reaction window.

The binding energies of the actual quantum states are calculated via self-consistent Hartree-Fock calculations using the COWAN-code (Cowan 1981). In figures 4.1 and 4.2 we have indicated the range of electron energies which result from these calculations for various two-electron configurations. Also we have included in figure 4.1 several of the relevant reaction windows. The {11} window for H_2 is shifted by 12 eV to lower electron energies and is considerably broader as compared to that for an Ar target (16 eV for Ar versus 23 eV for H_2). This is caused by the higher electron binding energies in H_2. But approximately the same projectile states can be expected to be populated. From figure 4.2 one might therefore surmise that for an Ar target electrons in the range of 0-20 and 70-95 eV originate from two-electron capture while electrons in the range 20-55 eV result from multi-electron capture. In the following we will show that this expectation is only partly true.

4.4.2 Two-electron capture

For two-electron capture the most probable binding energies of the first and second captured electron are calculated to be 28.8 and 42.2 eV. Capture will therefore predominantly take place into the $(n_1, n_2) = (4, 4)$ configurations. The corresponding autoionization electrons are indeed observed around 90 eV (see figure 4.5, upper panels).

In the 2+ coincident spectra of figure 4.5 at collision energies 35 keV and 70 keV we have drawn the reaction windows for the string {11} in N^{7+} collisions on Ar. It overlaps the (4,4) manifold and the (3,n), n >5, series of N^{5+} and for autoionization to the n=2 continuum of N^{6+} it is centered around an electron energy of 95.7 eV. From the shape of the window we would expect to see a decrease in the intensities of the (3,n) configurations for lower n. This is not the case. The most striking and unexpected feature in the 2+ coincident spectra of figure 4.5 is the occurrence of an intense N^{5+}(3,4) peak around 60 eV and the two less intense (3,3) and (3,5) peaks around 30 eV and 70 eV respectively. All these peaks lie far outside the calculated reaction window {11}, corresponding to capture of the two most loosely bound electrons. Although the (3,4) configurations are seen to be populated also for a H_2 target, there are significant differences: (a) in view of the different widths of the corresponding reaction

windows the (3,4) peak is much further outside the reaction window in the case of an Ar target, and (b) as opposed to H_2 the (3,4) configurations are even more strongly populated than the (3,5) configurations, although the latter are closer to the center of the reaction window. In the following we will discuss two possibilities to explain this experimental finding: (i) a post-collision interaction induced population transfer from (4,4) to (3,n) configurations as suggested by Bachau *et al* (1992), and (ii) three-electron processes with two-electron capture and simultaneous target excitation.

According to Hartree-Fock calculations 75 out of the 84 states with a (4,4) configuration have energies below the n=3 continuum of N^{6+} and can therefore interact with the (3,n) Rydberg series for $n > 9$. Moreover, as was pointed out by Bachau *et al* (1992) and as can be seen from the potential curve diagram of figure 4.6, at small internuclear distances a coupling is possible between (4,4) configurations and the (3,n) series even for $n \leq 9$. This is caused by the different slopes of the corresponding potential curves (in figure 4.6 we have assumed $10/R$ Coulomb curves for the (4,4) manifold and $12/R$ curves for the (3,n) series).

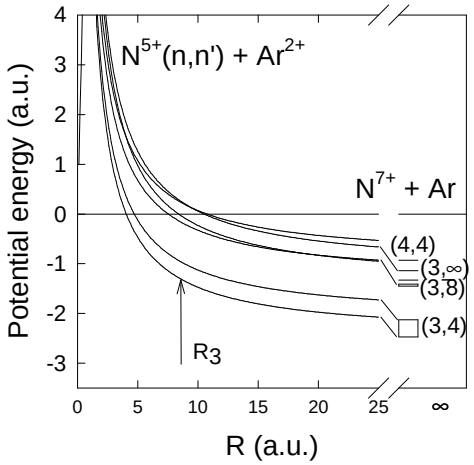

Figure 4.6: Potential energy curves for different cases of two electron capture. R_3 is the distance where three-electron capture can take place as calculated from the overbarrier model.

However, as long as only two electrons are supposed to become quasi-molecular during the collision, only internuclear distances R>8.6 a.u. should be considered, because according to the overbarrier model the third target electron becomes quasi-molecular at smaller distances. The lowest member of the (3,n) Rydberg series which can interact with the (4,4) manifold is then the (3,7) configuration. A population of (3,4), (3,5) and (3,6) configurations in N^{5+} is therefore not possible with the assumption of only two 'active' electrons.

These considerations lead us to leave the two-electron assumption and also to consider three-electron processes, characterized by the strings {110}, {101} and {011}. All three imply sufficiently small impact parameters for three Ar

target electrons to become quasi-molecular, but the third, second or first electron, respectively, is recaptured by the target such that only two electrons are transferred to the projectile. The corresponding reaction windows are indicated in figure 4.1. Those for the strings {011} and {101} are shifted with respect to that for {110}. Also the windows are wider than that for {11} due to the smaller impact parameter. The most probable binding energy of the recaptured electron e.g. for the {011} string is calculated to be 22.7 eV and thus is much less than the 40.7 eV of the ground state of Ar^{2+}. This implies that the target ion is formed in an excited state which will decay by photon emission. In figure 4.1 one can see that the reaction window for the {011} string now partly overlaps the electron peaks due to decay of the N^{5+}(3,4) manifold and we suggest that population of the (3,4) configuration in double capture processes is accompanied by target ion excitation. Target excitation in a similar way has also been observed in e.g. collisions of C^{4+} and N^{5+} on He (Hoekstra *et al* 1993).

Although the fact that the (3,4) configuration is populated can be understood qualitatively in this way, its relatively high intensity is still amazing. However, regarding the relative spectral intensities of the various states populated by two-electron capture one has to keep in mind that their respective branching ratios for autoionizing decay are significantly different. It is well known that autoionization rates of asymmetric configurations (3,n) decrease with increasing n. These states stabilize radiatively with a high probability. Statistically the high-ℓ states are preferably populated and their most probable decay is along the yrast-chain, in which the inner electron $(n, l = n-1)$ decays to $(n' = n-1, l' = n-2)$ (Ali *et al* 1993, Cederquist *et al* 1992). In this way autoionization is impeded and this implies that the measured relative intensities of the various (3,n) peaks in our spectra do not directly reflect the relative populations of the corresponding states. The actual population of the (3,n) states is underrepresented in our spectra, especially for higher n-values.

Experimental evidence for radiative stabilization has been obtained by several groups (Roncin *et al* 1991, Ali *et al* 1993, Martin *et al* 1993). A quantitative measurement of the fraction of two-electron transfer processes, which lead to radiative stabilization as opposed to a subsequent autoionization has been performed by Roncin *et al* (1991) by means of coincident projectile-target spectroscopy. For N^{7+} on Ar collisions at 10.5 keV they find that at least 30% of the two-electron transfer processes undergo a radiative stabilization. For an interpretation of this fraction they assume a primary transfer of electrons exclusively into (4,4) configurations. In the light of the new coincidence measurements presented here it should be taken into account that there is another important reaction channel, leading to (3,4) population. Together with the simultaneous target excitation this channel has almost the same inelastic energy loss and can therefore not be distinguished from the (4,4) channel in the energy gain spectra measured by Roncin *et al* (1991). Since radiative stabilization of (3,4)-states is negligible this implies that the fraction of (4,4) capture transferred to radiatively stabilizing (3,n), $n > 9$, configurations is even larger than anticipated by Roncin *et al* (1991).

Several suggestions have been made in the literature regarding the mechanisms responsible for the population of the various (3,n) configurations with high n. So called direct mechanisms, where configuration interactions between the different symmetric and asymmetric configurations are invoked for a direct population of these mixed states were suggested by Chen and Lin (1993), Vaeck and Hansen (1993), and Vaeck *et al* (1993). Stolterfoht *et al* (1990) discussed a direct correlated double capture during the formation of the quasi-molecule. Bachau *et al* (1992) suggested the mechanism based on post collision interaction which was mentioned above, see also Roncin *et al* (1993).

4.4.3 Three-electron capture

The reaction windows for two, three and four-electron capture are drawn in figure 4.7. The overbarrier model predicts for three-electron capture, string {111}, a total binding energy of 121 eV. Moreover we have indicated in this figure the calculated binding energies for certain configurations. We see that the (3,n_2,n_3) configurations are preferentially populated, as was already pointed out by Benoit-Cattin *et al* (1988).

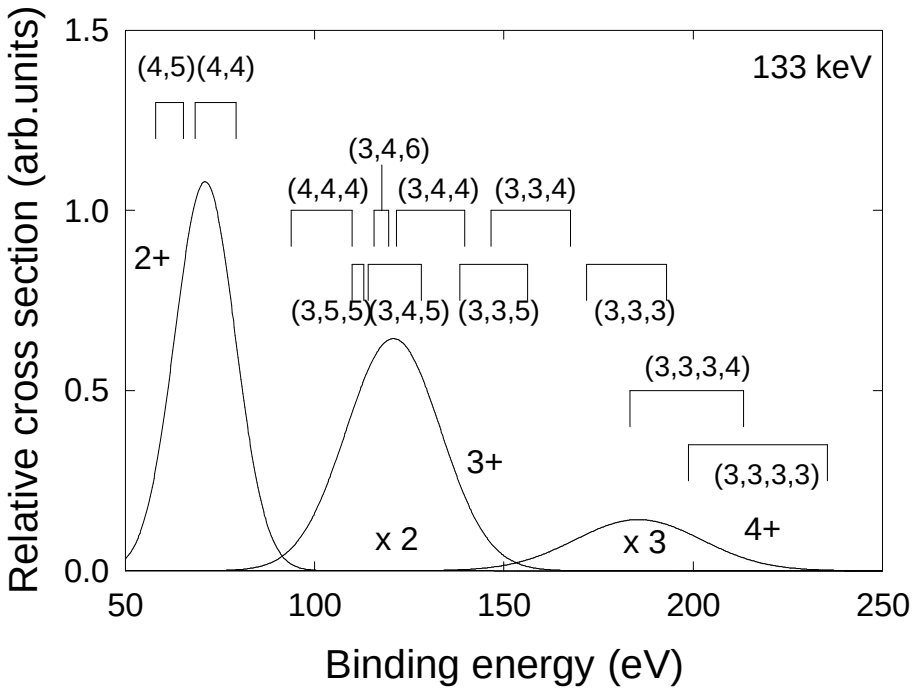

Figure 4.7: Reaction windows calculated from the overbarrier model for capture of two, three and four electrons during 133 keV N^{7+}-Ar collisions. Indicated above the reaction windows are the calculated binding energies for various configurations.

We also observe that the reaction window overlaps the (4,4,4) configurations.

The binding energies lie between 93.7 and 109.9 eV. The overbarrier model predicts for the classical principal quantum number 3.6, 3.5 and 3.5, respectively so it is possible that a small fraction of the electrons will be captured in the symmetric (4,4,4) level, as calculated from equation (4.2).

The (4,4,4)→(2,4,ϵ) transition yields autoionization electrons in the energy range of 86.1 to 106.9 eV. This is a somewhat broader range than that of (4,4)→(2,ϵ) transitions. In the central panel of figure 4.5 autoionization electrons in coincidence with three-electron capture, we see indeed a small contribution of three-electron capture in this energy range. Furthermore we must point out that this intensity is even higher in the 133 keV coincidence measurements (not shown here). This can be ascribed to the fact that the reaction window will be broader at higher collision energies so the population will increase for higher energies. The other transitions (4,4,4)→(3,4,ϵ) yield autoionization electrons in the range 0 to 16.6 eV as a first step. The (3,4) configurations will then decay to (2,ϵ) yielding autoionization electrons in the range 56 to 66 eV. Indeed we see in the partial spectrum of figure 4.5 autoionization electrons in that range.

The population of the (3,4,n_3) series leads to autoionization electrons in the energy range 0 to 40 eV for transition to (3,3,ϵ). The following step is then (3,3)→(2,ϵ) yielding autoionization electrons between 26.8 and 41.2 eV indicated as (3,3) in figure 4.1. The transition to (2,4,ϵ) yields electrons in the range from 60 to 100 eV. Most of these states, lying in the reaction window, emit first step autoionization electrons with kinetic energies from 0 to 100 eV.

4.4.4 Four-electron capture

For four-electron capture the overbarrier model predicts a total binding energy of 183 eV for the string {1111}. The most probable principal quantum numbers are calculated to be (3,3,3,3). The calculated binding energies for such states lie in the range (234;198) eV. Decay to (2,3,3) with binding energies in the range of 279-256 eV yields autoionization electrons between 22 eV and 81 eV. Subsequent decay will probably lead to (2,2,ϵ) resulting in autoionization electrons between 10 and 55 eV. Four-electron capture therefore results in a wide range of energies of the first and second electrons in the cascade.

Because there are hundreds of fourfold excited states the electrons resulting from the first step of the autoionization cascade form almost a continuous spectrum. In this context it is noteworthy that for N^{7+} colliding on Ar the spectra (cf. figure 4.1) show for example electron intensities between the (3,3) and (3,4) peaks, which are not present for collisions on H_2. The second step electrons yield lines which are more resolved because the binding energies of the different configurations vary over a smaller energy range.

4.5 Conclusions

We succeeded in measuring autoionization electrons from collisions of $^{15}N^{7+}$ on Ar in coincidence with the charge state of the target, providing partial electron

spectra. These first bare-ion coincidence spectra have been analyzed in the framework of the classical overbarrier model.

In the case of pure two-electron capture we observed that the assumption that only the most loosely bound electrons in Ar are involved during the transfer of two-electrons (i.e. the string {11}) could not account for the observed intensities of the (3,n) configurations, as shown in figure 4.5, upper panel. Our results suggest that three-electron processes with two-electron capture accompanied by target-ion excitation play an important role for populating the lower (3,n), $n > 3$ configurations.

Although the populations of the (3,n) configurations could be described in the framework of the overbarrier model assuming target excitation, it turned out that the population of the asymmetric (3,n) series and the (4,4) manifold is underrepresented in our spectra due to the possibility of radiative stabilization of these series. Stabilization would suggest that the inner electron decays radiatively and will end up in (2,n) and subsequently to (1,n) and can therefore not contribute to the observed intensities of the (3,n). Regarding the (4,4) manifold our results imply that radiative stabilization plays an even larger role than was concluded from the projectile-target ion coincidence measurements of Roncin *et al* (1991).

Three- and four-electron capture processes seem to be well described by the overbarrier model as can be seen from the overlap of the reaction window with the observed states. It turned out that in the range from 0 to 95 eV the measured electrons not only result from the first autoionization cascade, but also from the second and (if possible) the third step in the cascade.

References

Ali R, Cocke C L, Raphaelian M L A and Stö M 1993 *J. Phys. B: At. Mol. Opt. Phys.* **26** L177

Bachau H, Roncin P and Harel C 1992 *J. Phys. B: At. Mol. Opt. Phys.* **25** L109

Benoit-Cattin P, Bordenave-Montesquieu A, Boudjema M, Gleizes A, Dousson S and Hitz D 1988 *J. Phys. B: At. Mol. Opt. Phys.* **21** 3387

Bordenave-Montesquieu A, Benoit-Cattin P, Boudjema M, Gleizes A and Bachau H 1987 *J. Phys. B: At. Mol. Opt. Phys.* **20** L695

Cederquist H, Andersson H, Beebe E, Biedermann C,Broström L,Engström Å, Gao H, Hutton R, Levin J C, Liljeby L, Pajek M, Quinteros T, Selberg N and Sigray P 1992 *Phys. Rev.* A **46** 2592

Chen Z and Lin C D 1993 *J. Phys. B: At. Mol. Opt. Phys.* **26** 957-963

Cowan R D 1981 *The Theory of Atomic Structure and Spectra* (University of California Press, Berkley, 1981)

Geller G and Jacquot B. 1982 *Nucl. Instrum. Meth* **202** 299

Hoekstra R, Beijers J P M, De Heer F J and Morgenstern R 1993 *Z.Phys.D.* **25** 209

Mack M 1987a Rijksuniversiteit Utrecht *Thesis*

Mack M 1987b *Nucl. Instrum. Methods* **B23** 74-85

Mack M and Niehaus A 1987 *Nucl. Instrum. Methods* **B23** 109, 116, 291

Martin S, Denis A, Delon A, Désesquelles and Ouerdane Y 1993 *Phys. Rev.* A **48** 1171

Niehaus A 1986 *J. Phys. B: At. Mol. Phys.* **19** 2925

Olson R E 1981 *Phys. Rev.* A **24** 1726

Posthumus J H 1992 Rijksuniversiteit Groningen *Thesis*

Posthumus J H and Morgenstern R 1992a *Phys. Rev. Lett.* **68** 1315

Posthumus J H and Morgenstern R 1992b *J. Phys. B: At. Mol. Opt. Phys.* **25** 4533

Posthumus J H, Lukey P. and Morgenstern R 1992 *J. Phys. B: At. Mol. Opt. Phys.* **25** 987
Roncin P, Gaboriaud M N and Barat M 1991 *Europhys. Lett.* **16** 551
Roncin P, Gaboriaud M N, Barat M, Bordenave-Montesquieu A, Moretto-Capelle P, Benhenni M, Bachau H and Harel C 1993 *J. Phys. B: At. Mol. Opt. Phys.* **26** 4181
Stolterfoht N, Sommer K, Swenson J K, Havener C C and Meyer F W 1990 *Phys. Rev.* A **42** 5396
Vaeck N and Hansen J E 1993 *J. Phys. B: At. Mol. Opt. Phys.* **26** 2977
Vaeck N, Van der Hart H W and Hansen J E 1993 *Proc. VIth Int. Conf. on the Physics of Highly Charged Ions. (Manhattan, KS 1992)*(New York:AIP,1993)